



“Gheorghe Asachi” Technical University of Iasi, Romania



## PORE STRUCTURE CHARACTERIZATION OF CHEMICALLY MODIFIED BIOCHAR DERIVED FROM RICE STRAW

Sobhy M. Yakout<sup>1,2\*</sup>, Abd El Hakim M. Daifullah<sup>2</sup>, Sohair A. El-Reefy<sup>2</sup>

<sup>1</sup>King Saud University, College of Science, Biochemistry Department, Riyadh 11451 Saudi Arabia

<sup>2</sup>Atomic Energy Authority, Hot Laboratories Centre, 13759, Egypt

### Abstract

Biochar derived from agricultural biomass waste is increasingly recognized as multifunctional material for various applications according to its characteristics. It is therefore essential to investigate biochar properties before large-scale application. In this study, rice straw-derived biochars produced at different temperatures (550, 650, 750 °C). The resulting biochars were subjected to liquid-phase oxidation by different agents including KOH, HNO<sub>3</sub>, H<sub>2</sub>SO<sub>4</sub>, H<sub>2</sub>O<sub>2</sub> and KMnO<sub>4</sub> to obtain biochar with different properties. Pore structure characteristics including surface area, micro and meso pore volume, and pore size distribution were studied. Biochar surface is sensitive to the type of modifying reagent. Biochars treated by KOH, KMnO<sub>4</sub> and H<sub>2</sub>O<sub>2</sub> give higher nitrogen uptake in the range of micropores and mesopores. The rice straw-derived biochars especially produced at 650°C and treated by KOH have the highest surface area (179.7 m<sup>2</sup>/g) and micropore volume (0.081 cc/g) than the rest of biochars. In contrast, biochars treated by H<sub>2</sub>SO<sub>4</sub> and HNO<sub>3</sub> give lower nitrogen uptake and lead to loss of the biochar's porosity. Loss of micropore volume is as low as 10-40% of pore volume in H<sub>2</sub>SO<sub>4</sub> and HNO<sub>3</sub> treated biochars. Biochars exhibit wide pore size distribution, from narrow micropores to wide mesopores. One modal distribution was obtained with peak oscillation in the region of 1.0 to 1.3 nm in the case of micropore region. However, for mesopore region, two minima at about 3.0 nm and 5.0 nm were observed. More homogenous micropore distribution was produced from KOH and H<sub>2</sub>O<sub>2</sub> treatment in contrast to that of HNO<sub>3</sub> and H<sub>2</sub>SO<sub>4</sub> treatment, which give heterogeneous micropore distribution.

*Key words:* activated biochar, pore size distribution, pore volume, rice straw, surface area

*Received:* March, 2013; *Revised final:* April, 2014; *Accepted:* April, 2014

### 1. Introduction

Biomass is a renewable energy resource and has a growing interest as a chemical feedstock source. The pyrolysis conversion of biomass into value-added products namely; solid char (bio-char), liquid (bio-oil) and gas (bio-gas) has attracted tremendous research interest, mainly due to the rising energy demands and concerns over greenhouse gas emissions (Heo et al., 2010). Many applications used the liquid product (bio-oil), however no attention has been received for char.

Biochar is a new scientific term with various definitions in the literature. On the word of Lehmann and Joseph (2009), biochar can be well-defined as “a

carbon rich product when biomass such as wood, manure or leaves is heated in a closed container with little or unavailable air”.

Shackley et al. (2012) described biochar in more words as “the porous carbonaceous solid produced by the thermochemical conversion of organic materials in an oxygen depleted atmosphere that has physicochemical properties suitable for safe and long-term storage of carbon in the environment”.

Indeed, various types of biomass containing animal wastes, crop residues and sewage sludge used to prepare useful biochars via slow to intermediate pyrolysis processes (Ahmad et al., 2014). Agricultural wastes or residues are wide available low-cost raw material to produce biochar, as well as

\* Author to whom all correspondence should be addressed: e-mail: sobhy.yakout@gmail.com; Phone: +966558448693; Fax: +96614675931

biooil and gases (Chen et al., 2011a).

Rice straw is one of the main categories of agricultural by-products. Large quantities of straws accumulate due to agricultural practices in Egypt. Although some residues are used as feed, fuel or straw returned to the fields, millions of tons of rice straws are burnt annually in Egypt through wildfires, post-harvest burning of cultivation fields, and domestic uses for cooking and heating. This represents a main source of source of air pollution.

The main harmful of burning agricultural by-products is carbon dioxide gas emission. Carbon dioxide gas is considered as the most significant greenhouse gas created by human activities. Pyrolysis of straw agricultural wastes to give charcoal and biochar like product has been proposed to decrease undesirable effects of direct burning on human health and environment. As result of the biochar is opposing to biological decomposition, it is remain for much longer time in the terrestrial systems and then their useful effects are prolonged (Lehmann et al., 2011).

In the past five years, several researchers began to focus on developing biochar from straw (Chen et al., 2011b; Hameed and El-Khaiary, 2008; Lima et al., 2010; Qiu et al., 2009; Sun et al., 2011; Xu et al., 2011). However, limited knowledge is available for the surface modification of biochar. The surface modifications result in variation of surface reactivity, physicochemical and structural properties.

Surface modification of biochar using alkali or acid results in changing of surface areas plus functional groups characteristics on biochar. Further investigation on biochar modification is important owing to necessity to develop it for special application.

Bio-char has various applications for soil amendment, removal of toxic materials and production of value-added products (Azargohar et al., 2014). To evaluate each type of bio-char for any particular application, the bio-char should be characterized for its composition, porous structure and surface chemistry (Azargohar et al., 2014).

The objectives of this work consist in the examination of the modification of biochar prepared from Rice straw by using various liquid-phase oxidation methods, the investigation of the

modification effects on the pore structure and surface properties of the products, and the determination of the optimum experimental conditions for the preparation of materials with desired surface properties and adsorption capacities

## 2. Experimental

### 2.1. Preparation of biochar

Rice straw biochar was prepared according to our previous study (Daifullah et al., 2007), briefly, dried Rice Straw (500 gm) was heated at 50°C/10 min in fluidized bed reactor under flow 300ml/min of nitrogen. When temperature reached 350 °C, steam at a rate of 5 ml/min was introduced. Heating continued up to 550, 650, 750 °C, with one hour hold. After cooling, biochars were left to cool, washed with distilled water, and dried at 120 °C. Biochar at 550, 650 and 750°C took the abbreviations of RS<sub>1</sub>, RS<sub>2</sub>, and RS<sub>3</sub> respectively.

#### 2.1.1. Oxidative modification of biochar (RS<sub>1</sub>, RS<sub>2</sub>, RS<sub>3</sub>)

Obtained biochars were subjected to liquid-phase oxidation using different oxidizing agents in order to obtain materials with various surface characters.

The experiemntail procedures using different oxidizing agents were summarized in Table 1. After each modification biochar then washed with deionized water, decanted and the samples were dried overnight in an oven at 110 °C and stored in a desiccator for latter use.

### 2.2. Pore structure characterization

In order to determine surface areas and pore characteristics of various samples, nitrogen adsorption/desorption isotherms were measured at 77 K on an automatic adsorption instrument (Quantachrome Instruments, Model Nova1000e series, USA) in relative pressure in the range of 10<sup>-6</sup> to 0.999. Before measurement, biochar samples were crushed and powdered to shorten the time required for reaching equilibrium in the isotherm study and degassed at 250°C under nitrogen flow for 16 hours.

**Table 1.** Experimentail procedur for modification of RS biochars by different agents

<i>Agent</i>	<i>Procedure</i>	<i>Symbole</i>
KOH	RS biochars were treated with 1M KOHwith boiling for 2h. The oxidized biochars were washed and then dried over night at 50 °C (Shim et al., 2001).	RS <sub>1</sub> /KOH
HNO <sub>3</sub>	50g of RS biochars were treated with 50cm <sup>3</sup> of 65% nitric acid at 60 °C with stirring for 3 h (El-Hendawy, 2003).	RS <sub>1</sub> /HNO <sub>3</sub>
H <sub>2</sub> SO <sub>4</sub>	RS biochars were treated with 2% H <sub>2</sub> SO <sub>4</sub> (v/v) at 150 °C for 24 h. then washed with deionized water until pH was stable. Afterwards, the material soaked in 1% sodium bicarbonate solution overnight to remove residual acid (Babel and Kurniawan, 2004).	RS <sub>1</sub> / H <sub>2</sub> SO <sub>4</sub>
H <sub>2</sub> O <sub>2</sub>	RS biochars were immersed in 30% H <sub>2</sub> O <sub>2</sub> with a ratio of H <sub>2</sub> O <sub>2</sub> to RS of 10 ml /g at room temperature until complete degradation of the H <sub>2</sub> O <sub>2</sub> (when there was no further gas evolution)(Pereira et al., 2003).	RS <sub>1</sub> / H <sub>2</sub> O <sub>2</sub>
KMnO <sub>4</sub>	1g of RS biochars were treated by 50ml 0.1 N KMnO <sub>4</sub> solution at 50 °C for 48h (Youssef et al., 1982).	RS <sub>1</sub> / KMnO <sub>4</sub>

The cross section area, i.e the area occupied by an adsorbate molecule in completed monolayer for the N<sub>2</sub> molecule at 77K was taken as 16.2 Å<sup>2</sup>. The surface area of the biochar samples was obtained by means of standard methods, pore volume and pore size distribution were subsequently calculated from the N<sub>2</sub> adsorption data using NOVA Win 2.0 software. BET equation and Langmuir equation in the range of relative pressure 0.05 up to 0.3 was used to calculate the apparent surface area (S<sub>BET</sub>, S<sub>L</sub>).

The total pore volume (V<sub>t,0.95</sub>) estimated from amount of nitrogen adsorbed at relative pressure of 0.95 and the mean pore radius from  $r_{BET} = 2V_t/S_{BET}$ , assuming cylindrical pore opens at both ends (NOVAWin2 / 2-P Ver. 2.1 Operation Manual). DFT method was used to calculate the total surface area (S<sub>DFT</sub>) and total pore volume (V<sub>t,DFT</sub>) of investigated samples as well as those parameters of respective types of pore, e.g. the micropore, mesopore surface area (S<sub>mic,DFT</sub>, S<sub>mes,DFT</sub>), micropore and mesopore volume (V<sub>mic,DFT</sub>, V<sub>mes,DFT</sub>).

### 3. Results and discussion

#### 3.1. Nitrogen adsorption isotherms (comparative plots)

According to BDDT classification, the nitrogen isotherms in Fig. 1 are type I and IV with mesoporous hysteresis loop (Brunauer, 1943). In the present investigation, although the adsorption isotherms for all samples are similar, the adsorption capacities are significantly different according to the carbonization temperature and strength of modifying agent. In the case of samples treated by KOH, the upward shift is maximum in RS<sub>1</sub> and RS<sub>2</sub> series while samples oxidized by KMnO<sub>4</sub> give the maximum shift in RS<sub>3</sub> series. Only H<sub>2</sub>SO<sub>4</sub> treated biochars slightly shifted downward in all biochar series.

#### 3.2. Pore parameters analysis

It is clear from Table 2 that surface area resulting from micropores was over 80% of total surface area. It is well recognized that micropores are characterized by high surface area due to their tremendous number and depth (Girgis et al., 2002). The increase of temperature has a little effects on the surface area of products (RS<sub>1</sub>, RS<sub>2</sub>, RS<sub>3</sub>) while upon oxidation treatment the total surface area is highly increased using KOH followed by H<sub>2</sub>O<sub>2</sub> and KMnO<sub>4</sub>, whereas treatment with HNO<sub>3</sub> decreases the surface area while H<sub>2</sub>SO<sub>4</sub> treatment highly decreases the surface area. Decrease the micropore surface area in case of acid treatment due to great part of oxygen functional groups are located at the entrance of the pores, which hinder nitrogen molecules to go inside the pores (Pradhan and Sandles, 1999). According to Guo et al. (2005), the reduction of surface area is great in case of H<sub>2</sub>SO<sub>4</sub> treatment due to high

destruction effect results from the surplus water vapor released via H<sub>2</sub>SO<sub>4</sub> dehydration. This produce an over-gasification of parent biochar by converting micropores into meso- and macropores, and therefore causes a detrimental effect on the BET and micropore surface areas (Guo and Lua, 1999).

Table 2 show that Rice Straw based biochars prepared at 650 °C (RS<sub>2</sub>) give surface area little higher than that carbonized at 550 and 750 °C. These results are in good agreement with the total pore volume due to increasing micropore and mesopore volume. However, for carbonization temperatures higher than 650 °C the surface areas decreased due to the severe reaction of C-H<sub>2</sub>O and the burnt off of increased amount of biochar, resulting in the conversion of microporosities into mesoporosities or even macroporosities. Thus, carbonization at 650 °C can be considered as the temperature at which the reaction of steam with Rice Straw under our experimental conditions is the optimum. Pore-drilling and pore-widening by steam as a carbonizing agent occur simultaneously up to 650 °C to increase the micro and mesopore volumes. However, the pore-widening effect is more dominant by the gasification above 650 °C which destroys the pore wall of micropores (Yun et al., 2001). Upon increasing the temperature of carbonization the pore wide increases. Increasing temperature leads to the destruction of pore to larger one, increasing fraction percentage of mesopores and decreasing of micropores.

As can be seen from Table 2, there is a considerable increase in the pore diameter particularly for biochars modified by HNO<sub>3</sub>, H<sub>2</sub>SO<sub>4</sub> and KMnO<sub>4</sub>. This means that treatment of parent biochar leads to some destruction of micropores forming mesopores and increase pore diameter. The same results are supported when the fraction percentage of micropore and mesopores volume are compared. The fraction of micropore decreased especially in case of HNO<sub>3</sub> and H<sub>2</sub>SO<sub>4</sub>-oxidized samples, while mesopores fraction increased. The decrease of total surface area of samples treated by H<sub>2</sub>SO<sub>4</sub> and HNO<sub>3</sub> was mainly ascribed to the decrease of micropore volume i.e H<sub>2</sub>SO<sub>4</sub> and HNO<sub>3</sub> treatments result in extensive widening of the pores, breaking of pore wall and destroying of pore structure, leading to a decrease of surface area. Considering the parent samples as reference, the loss of micropore volume is as low as 10-40% of pore volume in nitric and sulfuric acid treated samples.

Thus, one can conclude that liquid-phase oxidation, especially when carried out under severe acidic conditions such as reported here, leads to the fixation of a large amount of oxygen functionalities on the biochar surface, with the simultaneous partial destruction or degradation of the porous structure of biochars.

Treatment by KMnO<sub>4</sub> leads to increase of mesopores and micropores volumes. Therefore, the micropore and external surface area are increased with subsequent increase of the total surface area.

This conformed by increasing pore radius from the parent samples but still lower than in case of acid treatments. For H<sub>2</sub>O<sub>2</sub>-treatment samples, a development of micropores and loss of mesopores volume are observed leading to increase of the micropore and the total surface area. This conformed by the reduction of pore radius. Similar results were obtained by Domingo-Garcia et al. (2000) and Korili and Gil (2001). In the case of KOH treatment, pore structure seems to depend on the carbonization

temperature of the parent samples. RS<sub>2</sub>/KOH has the highest surface area and micropore volume than all rest samples.

This means that its surface area concentrated in micropores. RS<sub>1</sub>/KOH has high micropore and mesopore volume that make the total pore volume reach its maximum in this sample while its micropore volume still lower than RS<sub>2</sub>/KOH so its surface area is lower than RS<sub>2</sub>/KOH but great compared to all other samples.

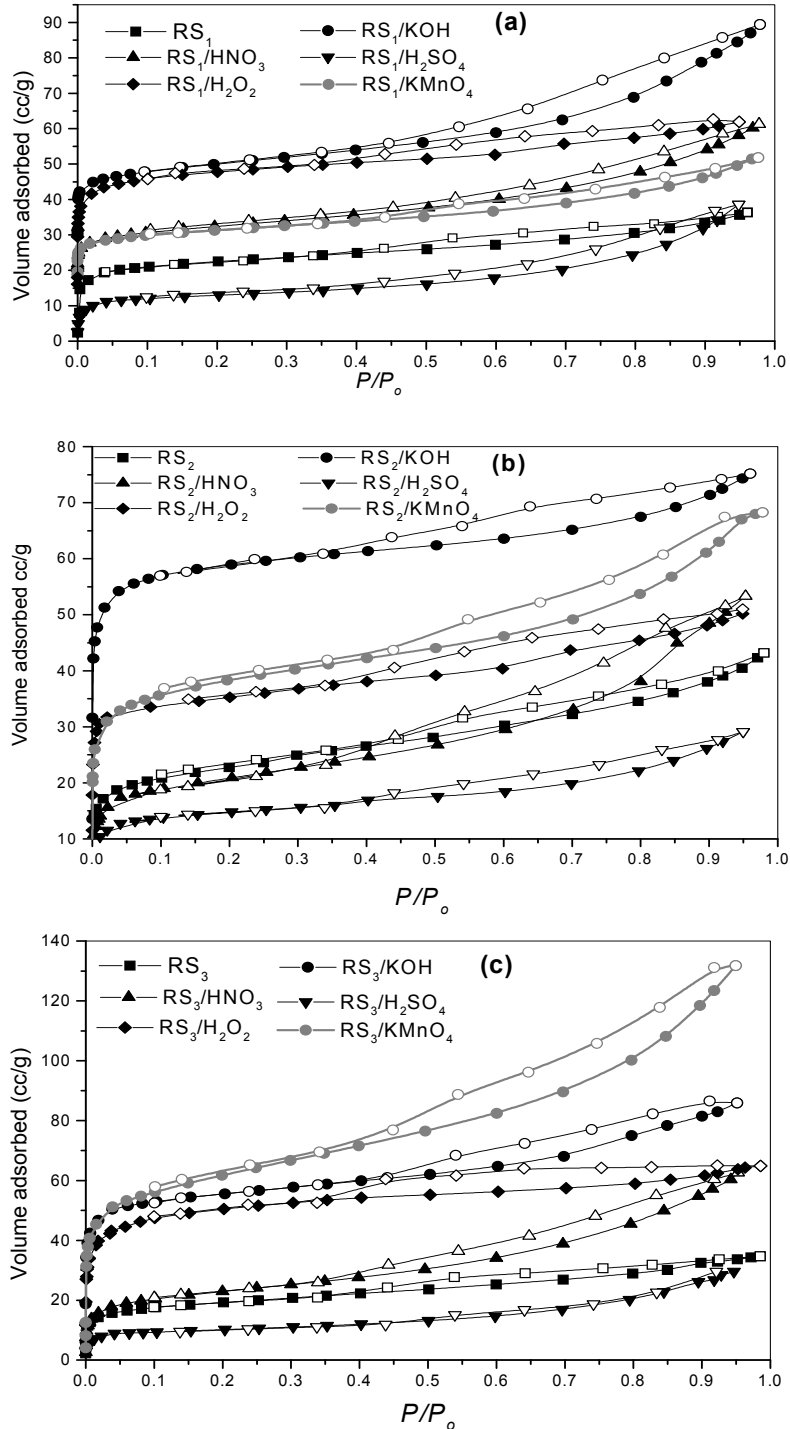
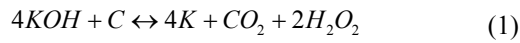


Fig. 1. (a) Nitrogen adsorption isotherms for RS<sub>1</sub> biochar series, (b) nitrogen adsorption isotherms for RS<sub>2</sub> biochar series and (c) Nitrogen adsorption isotherms for RS<sub>3</sub> biochar series (Solid symbols: adsorption; open symbols: desorption)

**Table 2.** Pore structure parameters of RS biochars

Method	BET			DFT					
	Residue	SBET (m <sup>2</sup> /g)	V <sub>p(0.95)</sub> (cc/g)	r <sub>BET</sub> (nm)	S <sub>DFT</sub> (m <sup>2</sup> /g)	S <sub>mic</sub> (m <sup>2</sup> /g)	S <sub>mes</sub> (m <sup>2</sup> /g)	V <sub>p(DFT)</sub> (cc/g)	V <sub>mic</sub> (cc/g,%)
RS <sub>1</sub>	71.35	0.055	1.55	59.5	51.5	8.0	0.054	0.03(55)	0.024(45)
RS1/KOH	143.3	0.175	2.45	137.1	100	37.1	0.165	0.065(25)	0.1(75)
RS1/HNO <sub>3</sub>	87.2	0.118	2.7	59.4	30	29.4	0.11	0.02(18)	0.09(82)
RS1/H <sub>2</sub> SO <sub>4</sub>	56.9	0.082	2.9	43.9	29.2	14.7	0.08	0.02(25)	0.06(75)
RS1/H <sub>2</sub> O <sub>2</sub>	110.9	0.078	1.4	107.3	98.0	9.3	0.076	0.05(66)	0.026(34)
RS1/KMnO <sub>4</sub>	87.75	0.095	2.2	71.6	51.3	20.3	0.094	0.03(32)	0.064(68)
RS <sub>2</sub>	76.2	0.063	1.6	65.3	52.8	12.5	0.064	0.034(53)	0.03(47)
RS2/KOH	179.7	0.115	1.3	186.6	180	6.4	0.105	0.081(77)	0.024(23)
RS2/HNO <sub>3</sub>	68.8	0.083	2.4	56.4	39.7	16.7	0.074	0.021(28)	0.053(72)
RS2/H <sub>2</sub> SO <sub>4</sub>	46.9	0.045	1.9	40.4	33.2	7.17	0.047	0.02(44)	0.025(56)
RS2/H <sub>2</sub> O <sub>2</sub>	96.8	0.06	0.9	120.9	97.5	23.4	0.057	0.05(88)	0.007(12)
RS2/KMnO <sub>4</sub>	122.9	0.1	1.7	114.1	99.2	14.88	0.099	0.05(50)	0.049(50)
RS <sub>3</sub>	63.0	0.052	1.65	53.8	43.6	10.2	0.047	0.02(47)	0.025(53)
RS3/KOH	86.3	0.066	1.5	85.1	77.4	7.75	0.063	0.04(63)	0.023(37)
RS3/HNO <sub>3</sub>	66.3	0.081	2.45	50.7	32.3	18.4	0.077	0.02(26)	0.057(74)
RS3/H <sub>2</sub> SO <sub>4</sub>	47.5	0.065	2.7	37.0	24.2	12.8	0.054	0.014(26)	0.04(74)
RS3/H <sub>2</sub> O <sub>2</sub>	85.1	0.053	1.2	76.5	71.4	5.1	0.051	0.04(78)	0.011(22)
RS3/KMnO <sub>4</sub>	91.5	0.092	2.0	78.1	60.6	17.5	0.086	0.032(37)	0.054(62)

It has been reported that metals, and specially potassium may be intercalate to the biochar matrix, resulting in increase of pore volume and alkali might catalyze this process (Martin-Gullon et al., 2004). The potassium hydroxide is reduced by the biochar producing potassium metal which is removed by washing (Lillo-Rodenas et al., 2003) (Eq. 1).



We can conclude that the highest modification effect is produced by KOH and its treated biochars have very important properties i.e. it posses higher surface area and micropore volume than other treated biochars.

Generally, modified biochars give different micro and mesopore concentration compared to the original biochar. It may be considered that pores are formed by etching the lattice by different etchants so different sizes of pores are formed. By the use of such modifying solutions the fixation of oxygen

groups on the wall of mesopores converting those previously classified as mesopores into micropores i.e micropores increased (Korili and Gil, 2001). Together with the process of oxygen fixation, there is indication that some pores were destroyed because of the loss of pore wall results in increase of mesoporosity. Change to the physical morphology of modified biochar depends on the strength of the oxidizing agent. In summation, sever oxidation practically destroy the porous structure of the original biochar due to erosion of the pore wall, while oxidation carried out in moderate condition promotes some modification in the original texture characteristics.

### 3.3. Pore size distribution

Figs. 2 and 3 depict DFT pore size distribution of the biochar samples. It is clear that the samples exhibit wide pore size distribution, from narrow micropores to wide mesopores.

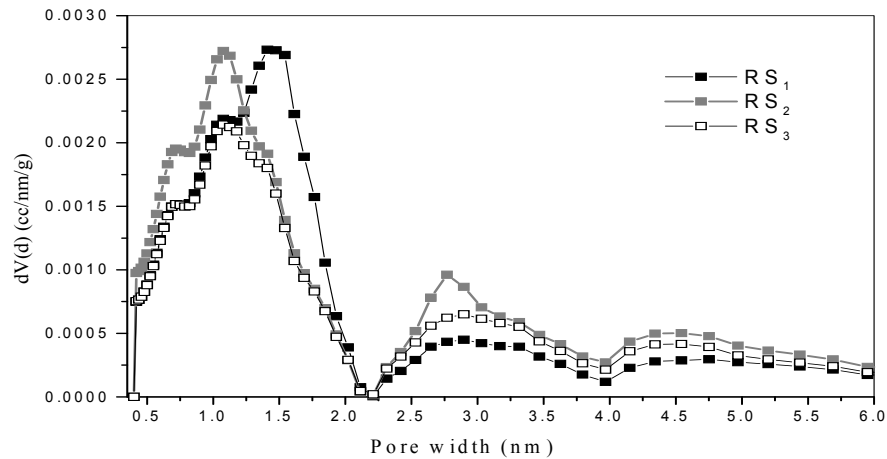


**Fig. 2.** DFT pore size distribution of biochar samples

Regarding of micropore region, one modal distribution of pore size is gained in all biochar samples with peak in fluctuate in range of 1.0 to 1.3 nm. For mesopore region, a wide pore size distribution was detected with two minima at about 3.0 nm and 5.0 nm corresponding to the transition from pore wide accommodating one adsorbed layer to two, and two layer to three, respectively (Villar-Rodile et al., 2002).

The results illustrate that carbonization temperature appears to affect pore size distribution (Fig. 2). The micropore of carbonized Rice Straw at 550 °C concentrated in peak at 1.5 nm while increasing carbonization temperature shifts this peak to lower pore width at 1.0 nm.

In mesopore range there are two broad peaks at 2.7 and 4.5 nm, its intensity increased by increasing carbonization temperature up to 650 °C.

Thus we can say that increasing carbonization temperature enhancing micro and mesoporosity.

The effect of increasing porosity with temperature occur up to 650 °C but by increasing temperature to 750 °C, there is remarkable contrast in the micropore volume and little decrease of mesopore volume. This indicates that increasing temperature above 650 °C lead to destruction of micropores and some mesopores. Thus Rice Straw carbonized at 650 °C has the highest developed micro and mesoporosity.

For samples treated by HNO<sub>3</sub> or H<sub>2</sub>SO<sub>4</sub> (Fig. 3), the micropore size distribution is destroyed by oxidation, with great reduction of micropore volume and shifting in direction of larger pore size in comparison with parent biochar, which is a highly pronounced with increasing carbonization temperature of the parent biochar.

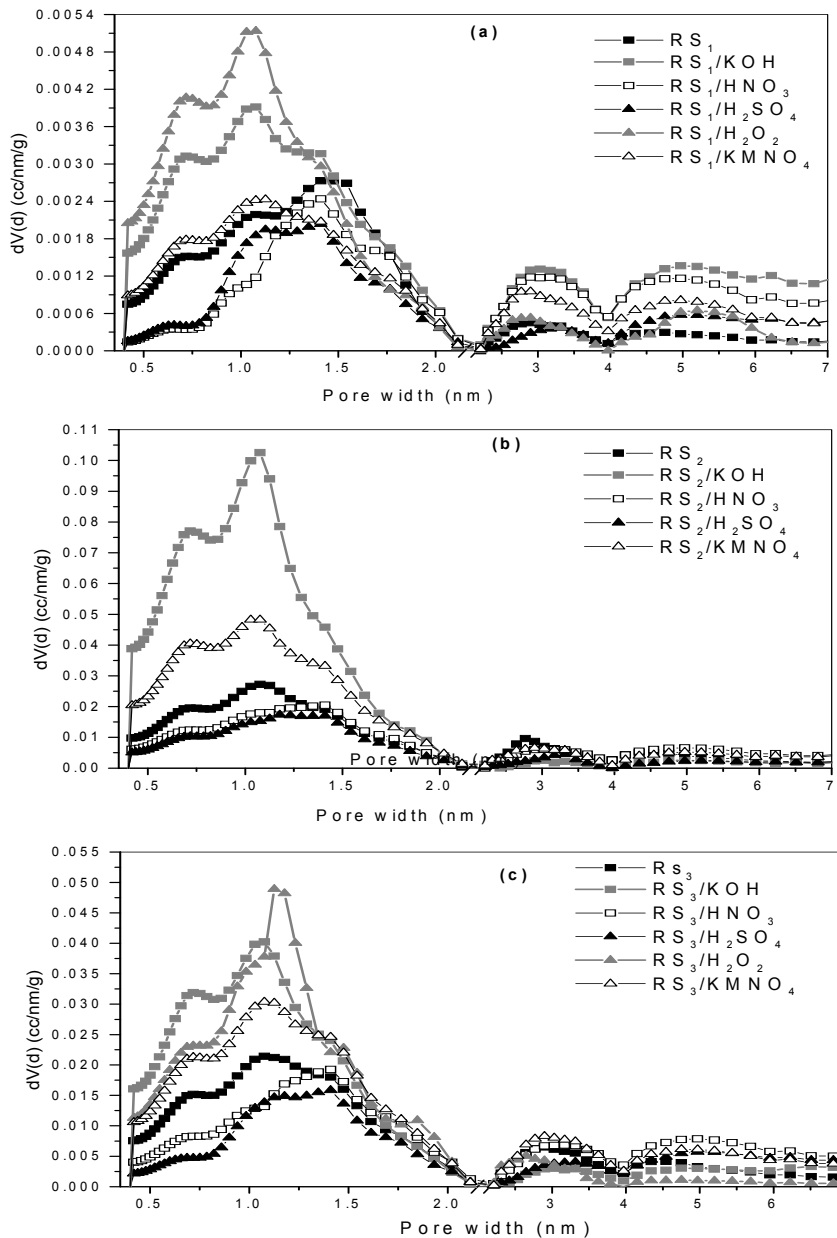


Fig. 3. (a) DFT pore size distribution of biochar samples (a) RS<sub>1</sub> series, (b) DFT pore size distribution of biochar samples (b) RS<sub>2</sub> series and (c) DFT pore size distribution of biochar samples (c) RS<sub>3</sub> series

In mesopore range, HNO<sub>3</sub> gives mesopores greater than H<sub>2</sub>SO<sub>4</sub> and this effect is highly appeared at high carbonization temperature where RS<sub>3</sub>/HNO<sub>3</sub> gives the highest mesoporosity of all samples.

Generally the peak height in case of HNO<sub>3</sub> treatment is greater than that of H<sub>2</sub>SO<sub>4</sub> treatment in both micropore and mesopore ranges. This means that the main effect of H<sub>2</sub>SO<sub>4</sub> treatments on microporosity is to open the preexistent pores while HNO<sub>3</sub> fix more oxygen groups converting mesopores to micropores, i.e. the destruction effect is predominate in H<sub>2</sub>SO<sub>4</sub> treatment while group fixation effect is predominate in HNO<sub>3</sub> treatment. This is probably one of the reasons why the mesopores volume increases in case of HNO<sub>3</sub> in spite of it has comparable micropore volume with H<sub>2</sub>SO<sub>4</sub> treatment.

In contrast, in the KOH and H<sub>2</sub>O<sub>2</sub> treatment, the micropore peak height increases which reflect the enhancement of micropore volume. Especially at lower carbonization temperature the peaks of KOH and H<sub>2</sub>O<sub>2</sub> are shifted to lower micropore diameter and KOH gives the greatest contribution of mesoporosity. So we can conclude that HNO<sub>3</sub> and H<sub>2</sub>SO<sub>4</sub> treatment give high developed mesoporosity, H<sub>2</sub>O<sub>2</sub> give highest microporosity while KOH give both high micro and mesoporosity.

The distribution of the peaks in samples treated by KOH and H<sub>2</sub>O<sub>2</sub> are sharper than that of the starting biochar, while the peaks of samples treated by HNO<sub>3</sub> and H<sub>2</sub>SO<sub>4</sub> are broader. These results indicate that more homogenous micropore distribution produced from KOH and H<sub>2</sub>O<sub>2</sub> treatment in contrast of HNO<sub>3</sub> and H<sub>2</sub>SO<sub>4</sub> treatment, which give heterogeneous micropore distribution (Korili and Gil, 2001).

In practice, more micropores are necessary for biochars application in gas phase adsorption because almost of gaseous pollutant molecules diameters range from 0.4 to 0.9 nm (Guo and Lua, 2000). On the other hand, biochars application for liquid phase adsorption must have mesopores owing to larger sizes of liquid molecules. This development in microporosities of biochars prepared from Rice Straw points to potential applications in both gas-phase and liquid-phase adsorption for air and water pollution control.

#### 4. Conclusions

Biochars porosity was significantly different according to the carbonization temperature and modifying agent strength. Under our experimental conditions 650 °C can be considered as optimum for biochar preparation. Surface area of biochars prepared at 650 °C (76m<sup>2</sup>/g) higher than that carbonized at 550 °C (71m<sup>2</sup>/g) and 750°C (63m<sup>2</sup>/g). Considering parent samples as reference, KOH treatment increases the surface area followed by H<sub>2</sub>O<sub>2</sub> and KMnO<sub>4</sub> whereas H<sub>2</sub>SO<sub>4</sub> decreases the surface area followed by HNO<sub>3</sub>. Increasing temperature shifts peak from 1.5 nm to lower pore

width at 1.0 nm and increases intensity of two peaks at 2.7 and 4.5 nm in mesoporous range.

#### Acknowledgments

The authors would like to extend their sincere appreciation to the Deanship of Scientific Research at King Saud University for its funding of this research through the Research Group Project No RGP-VPP-184.

#### References

- Ahmad M., Rajapaksha A.U., Lim J.E., Zhang M., Bolan N., Mohan D., Vithanage M., Lee S.S., Ok Y.S. (2014), Biochar as a sorbent for contaminant management in soil and water: A review, *Chemosphere*, **99C**, 19-33.
- Azargohar R., Nanda S., Kozinski J.A., Dalai A.K., Sutarto R., (2014), Effects of temperature on the physicochemical characteristics of fast 4 pyrolysis biochars derived from Canadian waste biomass, *Fuel*, **125**, 90-100.
- Babel S., Kurniawan T.A., (2004), Cr(VI) removal from synthetic wastewater using coconut shell charcoal and commercial activated carbon modified with oxidizing agents and/or chitosan, *Chemosphere*, **54**, 951-67.
- Brunauer S., (1943), *The adsorption of gases and vapors - Physical adsorption*, vol. I, Princeton University Press.
- Chen B., Chen Z., Lv S., (2011a), A novel magnetic biochar efficiently sorbs organic pollutants and phosphate, *Bioresource Technology*, **102**, 716-23.
- Chen X., Chen G., Chen L., Chen Y., Lehmann J., McBride M.B., Hay A.G., (2011b), Adsorption of copper and zinc by biochars produced from pyrolysis of hardwood and corn straw in aqueous solution, *Bioresource Technology*, **102**, 8877-84.
- Daifullah A.A., Yakout S.M., Elreefy S.A., (2007), Adsorption of fluoride in aqueous solutions using KMnO<sub>4</sub>-modified activated carbon derived from steam pyrolysis of rice straw, *Journal of Hazardous Materials*, **147**, 633-43.
- Domingo-Garca M., Lopez-Garzon F.J., Perez-Mendoza M., (2000), Effect of some oxidation treatments on the textural characteristics and surface chemical nature of an activated carbon, *Journal of Colloid and Interface Science*, **222**, 233-240.
- El-Hendawy A.A., (2003), Influence of HNO<sub>3</sub> oxidation on the structured and adsorptive properties of corncob activated carbon, *Carbon*, **41**, 713-722.
- Girgis B.S., Yunis S.S., Soliman A.M., (2002), Characteristics of activated carbon from peanut hulls in relation to conditions of preparation, *Materials Letters*, **57**, 164-172.
- Guo J., Lua A.C., (1999), Textural and chemical characterizations of activated carbon prepared from oil-palm stone with H<sub>2</sub>SO<sub>4</sub> and KOH impregnation, *Microporous Mesoporous Materials*, **32**, 111-117.
- Guo H., Lua A.C., (2000), Preparation of activated carbons from oil-palm-stone chars by microwave induced carbon dioxide activation, *Carbon*, **38**, 1985-1993.
- Guo J., Xu W.S., Chen Y.L., Lua A.C., (2005), Adsorption of NH<sub>3</sub> onto activated carbon prepared from palm shells impregnated with H<sub>2</sub>SO<sub>4</sub>, *Journal of Colloid and Interface Science*, **281**, 285-290.
- Hameed B.H., El-Khaiary M.I., (2008), Kinetics and equilibrium studies of malachite green adsorption on

- rice straw-derived char, *Journal of Hazardous Materials*, **153**, 701-708.
- Heo H.S., Park H.J., Yim J.H., Sohn J.M., Park J., Kim S.S., Ryu C., Jeon J.K., Park Y.K., (2010), Influence of operation variables on fast pyrolysis of *Miscanthus sinensis* var. *purpurascens*, *Bioresource Technology*, **101**, 3672-7.
- Korili S.A., Gil A.A., (2001), On the applications of various methods to evaluate the microporous properties of activated carbons, *Adsorption*, **7**, 249-264.
- Lehmann J., Joseph S., (2009), *Biochar for environmental management: an introduction*, Earthscans.
- Lehmann J., Rillig M.C., Thies J., Masiello C.A., Hockaday W.C., Crowley D., (2011), Biochar effects on soil biota –a review, *Soil-biology-and-biochemistry*, **43**, 1812–1836.
- Lillo-Rodenas M.A., Cazorla-Amoros D., Linares-Solano A., (2003), Understanding chemical reactions between carbons and NaOH and KOH, An insight into the chemical activation mechanism *Carbon*, **41**, 267–275.
- Lima I.M., Boateng A.A., Klasson K.T., (2010), Physicochemical and adsorptive properties of fast-pyrolysis biochars and their steam activated counterparts, *Journal of Chemical Technology and Biotechnology*, **85**, 1515-1521.
- Martin-Gullon I., Marco-Lozar J.P., Cazorla-Amoros D., Linares-Solano A., (2004), Analysis of the microporosity shrinkage upon thermal post-treatment of H<sub>3</sub>PO<sub>4</sub> activated carbons, *Carbon*, **42**, 1339–1343.
- Novawin2/2-P VER. 2.1, (2003), Operation Manual Quantachrome Instruments.
- Pereira M.F.R., Soares S.F., Órfão J.J.M., Figueiredo J.L., (2003), Adsorption of dyes on activated carbons: influence of surface chemical groups, *Carbon*, **41**, 811-821.
- Pradhan B.K., Sandles N.K., (1999), Effect of different oxidizing agent treatments on the surface properties of activated carbons, *Carbon*, **37**, 1323-1332.
- Qiu Y., Zheng Z., Zhou Z., Sheng G.D., (2009), Effectiveness and mechanisms of dye adsorption on a straw-based biochar, *Bioresource Technology*, **100**, 5348-5351.
- Shackley S., Carter S., Knowles T., Middelink E., Haeefele S., Sohi S., Cross A., Haszeldine S., (2012), Sustainable gasification-biochar systems? A case-study of rice-husk gasification in Cambodia, Part 1: Context, chemical properties, environmental and health and safety issues, *Energy Policy*, **42**, 49–58.
- Shim J.W., Park S.J., Ryu S.K., (2001), Effect of modification with HNO<sub>3</sub> and NaOH by pitch-based activated carbon fibers, *Carbon*, **39**, 1635-1642.
- Sun K., Ro K., Guo M., Novak J., Mashayekhi H., Xing B., (2011), Sorption of bisphenol A, 17alpha-ethinyl estradiol and phenanthrene on thermally and hydrothermally produced biochars, *Bioresource Technology*, **102**, 5757-5763.
- Villar-Rodile S., Denoye R., Rouquero J., Martinez-Alonso A., Tascon J.M.D., (2002), Porous Texture Evolution in Nomex-Derived Activated Carbon Fibers, *Journal of Colloid and Interface Science*, **252**, 169-176.
- Xu R.K., Xiao S.C., Yuan J.H., Zhao A.Z., (2011), Adsorption of methyl violet from aqueous solutions by the biochars derived from crop residues, *Bioresource Technology*, **102**, 10293-10298.
- Youssef A.M., Ghazy T.M., El-Nabaiuwy T.H., (1982), Moisture sorption by modified-activated carbons, *Carbon*, **20**, 113-116.
- Yun C. H., Park Y. H., Park C.R., (2001) Effects of pre-carbonization on porosity development of activated carbons from rice straw, *Carbon*, **39**, 559–567.